Synthesis of Nickel Sulfide Nanoparticles from Single Source Precursor (Metal Xanthate Complexes) Using Melting (Solvent-Less) Method

Abdulaziz A. Alanazi
Prince Sattam bin Abdulaziz University
Abdulrahman Alharthi
Prince Sattam bin Abdulaziz University
Fahad Abdulaziz
University of Hai'l
Salman Latif
University of Hai'l
Dina Salah
Ain Shams University
Elsayed M. Sherif
King Saud University
Moustapha E Moustapha (m.moustapha@psau.edu.sa)
Prince Sattam bin Abdulaziz University

Research Article

Keywords: stoichiometries, nanoparticles, X-ray, SEM, agglomerates, EDX analysis

Posted Date: November 3rd, 2021

DOI: https://doi.org/10.21203/rs.3.rs-1032431/v1

Abstract

Nickel sulfides are rich chemistry groups with discrete phases and stoichiometries, therefore they have various properties and applications. We herein prepare two single metal xanthate precursors [K(S_2COBu)] Potassium butyl xanthate and [K(S_2COPn)] Potassium pentyl xanthate using the melting method at two different temperatures 400 and 500°C to synthesize nickel sulfides nanoparticles. The nanoparticles were characterized using powder X-ray diffraction (p.XRD), energy-dispersive X-ray spectroscopy (EDX) and imaged using scanning electron microscopy (SEM). Two different nickel sulfides nanostructures obtained [Ni(S_2COBu)$_3$] and [Ni(S_2COPn)$_3$], the results from p.XRD show the sizes of the nanoparticles are (35.39±8.15 and 38.24±7.70 nm) at 400^{o}C respectively, and (43.12±4.52 and 47.45±4.22 nm) respectively at 500^{o}C. The result shows that the xanthate ligand affects the size of the nanoparticles as by increasing the alkyl chain length the size of the nanoparticles decrease. The (SEM) images show coral-like agglomerates, which are mainly assembled by spherical nanoparticles. EDX analysis shows stable and pure nickel sulfides with some variations in the elemental ratio of both nickel and sulfur according to the xanthate ligand used as a precursor to synthesis the nanoparticles. As a result, we introduce a simple, low cost and feasible synthesis of pure, stable, with definite size two nickel sulfides nanoparticles using metal xanthate ligands.

Introduction

An attractive target for many scientists due to the alterations in the optical[1], magnetic [2] properties and catalytic activities [3], which occur in nanometer-sized particles. Metal sulfides have a great feature prominently among the phases investigated in nanocrystalline form especially nanocrystals of CdS[4,5] and the wideband gap semiconductor ZnS.[6-8] Interestingly, the magnetic properties of other metal sulfide nanocrystals have been studied such as iron sulfide[9], nickel sulfide[10,11] phase systems, MnS, AgS [5], and numerous copper sulfide phases.[5,12]

Nickel II complexes are very important as they detect presences of pollutants, water vapour, and they have catalytic activates. They have unique optical, electrical properties and have different applications many studies report the high capacitance of the nickel sulfides such as Shombe and co-workers studies the conversion efficiency and specific capacitance of solvent-free synthesized different nickel sulfide composites. Their results are based on X-ray diffraction, transmission, and scanning microscopy[13]. Sajjad and Khan used nickel sulfide nanoparticles as electrode material for symmetric supercapacitor. The synthesized nanoparticles showed a uniform shape and size. Nickel sulfides electrodes showed enhanced electric properties such as high specific capacitance of 2495 F g^{-1} at 1 A g^{-1} and excellent cycling stability based on the Ragone plot shows a high energy density of 52.4 W h kg^{-1} and an ultra-high-power density of 13500.0 W kg^{-1}.[14]

Marand et al. studied electric properties of nickel sulfide reduced graphene oxide composite and reported a high specific capacitance of 305 Fg^{-1} at a current density of 1.1 A g^{-1} and high-capacity retention of

91% after 3000 cycles. The composite was synthesized using a solution combustion method. [15]

Nickel sulfides are also used as electrodes in the battery to enhance their electrical properties. Li et al. developed nickel sulfide nanoparticles with sulfur-doped reduced graphene oxide as dual-role anode materials for both lithium-ion battery (LIBs) and sodium-ion battery (SIBs) by increasing lithium and sodium storage efficiency. Their results showed good transition oxides/sulfides in alkali metal-ion batteries[16]. Li and co-workers synthesized a composite of nickel sulfide nanoparticles and reduced oxide nanosheets. The composites were synthesized via a simple one-step hydrothermal method using different temperatures. These composites avoided the agglomeration of the sodium ion batteries electrode materials and enhanced reversible capacity and better capability[17].

The photocatalytic activities of nickel sulfides also attracted many researchers Kumari and co-workers synthesized nickel sulfide nanostructures using the precipitation method. The surface of the nanostructure was functionalized and used for selective adsorption of anionic and cationic dyes and two different types of antibiotics. The adsorption of the dyes to the nanostructure was electrostatic, whereas the adsorption with the antibiotic was due to hydrogen bonding and metal coordination. The synthesized and functionalized nanostructure can be used as recyclable adsorbate for different organic pollutants[18]. Zhang and co-workers synthesized nickel sulfide composite for efficient photocatalytic nitrogen fixation upon sunlight irradiation. The composite system enhanced the electron transfer, increase the nickel sulfide band potential with the synergetic internal electric field and photogenerated electron-hole pairs. These results were confirmed by electrochemical impedance spectroscopy and photocurrent tests. The nickel sulfide composite system showed a good photocatalytic nitrogen reduction and produced a high NH_3 rate[19]. Dev and Singh studied nickel sulfide nanoparticles anchored graphene oxide among different metallic sulfide nanoparticles. Moreover, they tested the photocatalytic activates through methylene blue reduction[20]. Lakshmanan et al., synthesized nickel sulfides and nickel oxide nanoparticles using solvothermal and thermal decomposition, they characterized the synthesized nanoparticles by powder X-ray diffraction (pXRD), high resolution scanning electron microscopy (HRSEM), energy dispersive spectroscopy (EDS), and UV diffuse reflectance spectroscopy (UV-DRS). The photocatalytic activities of the nanoparticles were tested by detecting the degradation of methylene blue and rhodamine 6G upon UV irradiation. Their results showed that the nickel sulfide nanoparticles are more photocatalytic active than nickel sulfide nanoparticles[21].

As reported nickel II complexes are very important and have variable chemistry that let them applicable in different fields such as the detection of the presences of pollutants, water vapour, and they have catalytic activates. Nickle sulfides have been used in different applications such as agriculture [22], solar cells [23,24] and as superconductors [25], pollutants degradation[26].

The properties of nanoparticles mainly depend on their shape and size. According to different synthesis methods nanoparticles, different nanoparticles crystalline phases and sizes can be obtained. The different applications of synthesized nanoparticles depend on their precise synthesis and characterization. Using a single-molecule precursor has many advantages if compared to multi-source

synthetic protocols. Single molecules precursor synthesis resulted in constant and better composition nanoparticles and fewer crystal defects on its structure. Thus, a high-quality nanomaterial can be obtained. Synthesis of nickel sulfides using multi- sources is commonly used and reported in many studies[27-29]. Using a long organic chain was also reposted in many studies to control the size and morphology of the synthesized nanomaterials but they limit their application as they caused ligand surface chemistry complexity[30,31].

Many methods have been applied to synthesize metal sulfide nanocrystals such as hot injection[32–34] and colloidal methods[35], hydrothermal methods[36], solvothermal methods[37,38].

Solventless thermolysis method is distinguished over other routes their ease of synthesis in which solid-state decomposition of a precursor is accomplished by thermal treatment under inert conditions. The solventless thermolysis method is considered an effective way to synthesize metal chalcogenide nanomaterials with a wide range of morphologies such as nanorods[39], nanowires[40], nanospheres[41], and nanodisks[42]. Interestingly, melt thermolysis can provide a simple and cost-effective way to scale up production. Another advantage of this approach is its ability to offer economic and environmental benefits reduce the requirement for harsh materials, and typically, yields are frequently high. Melt reactions was used to synthesize a wide range of different nanoparticles materials including metal sulfides such as Bi_2S_3[43], Cu_2S[44], NiS[45], PbS[46], PdS[47] and CdS[48].

For single-source precursors, the origin of transition metals and non-metals materials of the target binary compound are associated with a single precursor species. Recently, this approach has been utilized widely in nanocrystal synthesis. Typically, it offers many great features such as ease of utilizing and high-quality products under relatively mild reaction conditions. [49-51] numerous transition metal sulfide nanocrystals have been synthesized using single-source precursors e.g., ZnS[52,53], iron sulfide[54,55], and nickel sulfide nanocrystals[56,57].

Xanthates (alkyl dithiocarbonates or ROCS-2) are organic compounds that contain two groups a negatively charged group that react with metals and a hydrocarbon chain that react with non-polar solvents. Xanthates complexes are applicable in different fields such as agriculture, antimicrobial industries, and material science[58]. Metal xanthates [$M(S_2COR)$ x] (M = transition metal, R = alkyl chain) are considered as a good choice to synthesis metal sulfides as they decomposed easily and cleanly at low temperatures[59]. In addition, it can be used as a capping ligand for the synthesis of metal nanoparticles and self-assembly monolayer. Using xanthates for the synthesis of nanoparticles have many advantages, as the by-products generated due to xanthates decomposition are highly volatile and can easily be removed from the reaction leaving a pure and stable nanoparticle.

Here we used the melting (solvent-less) method at two different temperatures 400 and 500°C to synthesis two nickel sulfide nanoparticles using two xanthate ligands [$K(S_2COBu)$] Potassium butyl xanthate and [$K(S_2COPn)$] Potassium Pentyl xanthate as a single-source precursor. Two nickel sulfides nanoparticles were characterized using XRD and EDX. The crystallite size (D) is calculated using the Debye-Scherrer

formula. The nanoparticles were imaged using SEM. We present a simple, low cost and feasible synthesis of pure, stable, with definite size two nickel sulfides nanoparticles using metal xanthate ligands.

Results And Discussion

Powder X-ray Diffraction (p.XRD)

The p.XRD patterns are shown in Figure.1. The peaks observed in the XRD pattern, which is a characteristic Bragg reflections at 2Θ values 30.25°, 32.18°, 34.50°, 35.66°, 37.30°, 40.40°, 45.61°, 48.76°, 50.06°, 52.53°, 53.34°, 56.23°, 57.40°, 59.60° and 72.53°

are corresponding to the planes with Miller indices (422), (402), (512), (611), (630), (541), (801), (303), (520), (413), (641), (802), (740), (911) and (621), respectively for nickel sulfide nanoparticles $[Ni(S_2COBu)_3]$ (Complex 1).

As shown in figure 1, the intensity of the peaks at 35.66° and 45.61° decrease with the increase of the temperature this change in the intensity is related to the size changes at a different temperature, also the two peaks 52.53° and 53.34° at 400°C almost merge to form one peak at 500°C as the size of the complex changes. This is due to different phase structures resulting as the temperature changed as previously reported by Roffey and coworkers[60].

Figure 2 represents the p.XRD of second nickel sulfide nanoparticles $[Ni(S_2COPn)_3]$ (Complex 2), peaks observed in the p.XRD pattern are the same as the one obtained for (complex 1). The peaks at 32.18° and 34.50° as well as the peaks at 52.53°, 53.34° at 400°C almost merged at 500°C, as discussed before due to different structure phases resulting from the temperature change. The peak at 34.50° at 400 disappears at 500 °C, which also confirm the structure phase changes at different temperature.

The crystallite size (D) is calculated using the Debye-Scherrer formula, the calculated crystallite size for $[Ni(S_2COBu)_3]$ nanoparticles was 35.39±8.15 at 400°C, and 43.12±4.52 at 500^{o}C, while for $[Ni(S_2COPn)_3]$ 38.24±7.70 and 47.45±4.22 for 400 and 500°C respectively. So, the size of the synthesized nickel sulfide decreases as the alkyl chain of the precursor increases. Buchmaier et al., who used two xanthate precursors at 180°C to synthesis nickel sulfide thin film, confirm our results. Their results confirm the synthesis changes reported 30 nm average size of the nickel sulfides forming the thin film[61].

Our results are in good agreement with the p.XRD pattern reported by Lakshman and coworkers for nickel sulfides nanoparticles, they reported a crystallite size 62 nm, they used solvent and thermal deposition method to synthesis nickel sulfide nanostructure[21]. Also, Almanqur et al. used xanthate single-source precursor to synthesis iron sulfides nanostructures by using spin coating and deposition methods, they reported different crystallite sizes using p.XRD according to different methods they used[62].

Some studies used the electrochemical method to synthesis nickel sulfide nanoparticles, they tested different experimental conditions and used maximum temperature at 60°C, their p.XRD showed α-phase nickel sulfide (JCPDS card no. 75-0613) and 19 nm average particles size[63]. Others used aerosol-assisted chemical vapour deposition at four different temperatures starting from 250 to 400°C to form a thin film of nickel sulfides, they used Bis(O-alkylxanthato) nickel (II), where the alkyls are hexyl and octyl. Their p.XRD results showed a mixture of hexagonal $Ni_{17}S_{18}$ and orthorhombic Ni_7S_6 nickel sulfide thin films[64].

Salavati-Niasari and coworkers used microwave radiation to synthesis nickel sulfide nanoparticles, and they tested different synthesis conditions as the effect of concentration of sulfur source, reaction time, and power of microwave irradiation. Their p.XRD results showed pure well-crystallized nickel sulfide nanoparticles.[65] Yu and Yoshimura used liquid-solid interaction between nickel and sulfur to synthesis nickel sulfide thin film and powder at a low temperature less than 250°C, there p.XRD results showed different nickel sulfide phases produced as different solvents were used to synthesis nickel sulfides[66].

Scanning electron microscopy (SEM)

The morphological features of the synthesized two nickel sulfide nanoparticles $[Ni(S_2COBu)_3]$ (1) and $[Ni(S_2COPn)_3]$ (2) are studied by scanning electron microscopic technique. Fig. 3 illustrates SEM images of two nickel sulfides nanoparticles obtained from two different xanthate ligands at two different temperatures. The SEM images of nickel sulfides nanoparticles showed agglomerated small bead-like structures forming coral-like shapes. These agglomerates are assembled by different shapes of nanoparticles.

Energy Dispersive X-ray Spectroscopy (EDX)

Further analysis of the synthesized nanostructures Energy-dispersive X-ray analysis was used to confirm the purity of the synthesized nanostructures through element analysis as shown in figure 4. The elemental composition obtained from EDX confirms a 1:1 ratio for the two nickel sulfides nanoparticles, for $[Ni(S_2COBu)_3]$ the ratio Ni% was (49.22 and 49.17) at 400 and 500°C respectively. Therefore, the nickel percentage is relatively less than S% (50.78 and 50.83) at the same temperatures sequence. However, for $[Ni\ (S_2COPn)_3]$ the Ni% was (50.32 and 50.60), which is slightly higher than S% (49.71 and 49.40) at 400 and 500°C respectively.

Conclusions

In this work, we used two single metal xanthate precursors $[K(S_2COBu)]$ Potassium butyl xanthate and $[K(S_2COPn)]$ Potassium pentyl xanthate and melting method at two different temperatures 400 and 500°C to synthesis two nickel sulfides nanoparticles complexes $[Ni(S_2COBu)_3]$ and $[Ni(S_2COPn)_3]$. The results show that the size and phase structure of the synthesized nickel sulfide nanoparticles are affected

by changing the temperature, also as the alkali chain length increases the size of the nickel sulfide nanoparticles decreases. The presented single source, solvent-less synthesis is a simple and low-cost method that produces pure, well crystallite nickel sulfide nanoparticles.

Methods

Materials

n-butanol (99.5%), n-pentanol (99.9%), carbon disulfide (99.9%), acetone (99.8%), poatassium hydroxide (99.5%) and nickel (III) nitrate (98%) were all acquired from Sigma-Aldrich and used without further purifications.

Synthesis of potassium n-butyl xanthate, [K(S2COnBu)] (Precursor 1-P1).

KOH (5.5 g, 98.04 mmol) was added to n-butanol and stirred. Then, carbon disulfide (CS_2) (7.56 g, 6.00 ml, 99.29 mmol) was added dropwise into the mixture. A yellow precipitate started to form, then precipitates were collected and recrystallized using acetone at room temperature and dried in the air. Elemental analysis for $C_5H_9KOS_2$ (%): calc: C, 31.89, H, 4.82, S, 34.01; K, 20.76; found: C, 32.16, H, 5.02, S, 33.80; K, 20.36. 1H NMR (400 MHz, D_2O): 4.66 (t, 3H, CH_2), 1.78 (m, 5H, CH_2) 1.41 (m, 6H, CH_2), 0.96 (t, 3H, CH_3).

Synthesis of potassium isopropyl xanthate, [K(S2COnPn)] (Precursor 2-P2)

Potassium n-pentyl xanthate was synthesized by following the same method for P1. $C_6H_{11}KOS_2$ (%): calc: C, 35.61, H, 5.48, S, 31.68; K, 19.32; found: C, 35.91, H, 5.82, S, 32.02; K, 19.53. 1H NMR (400 MHz, D_2O): 4.66 (t, 3H, CH2), 1.58 (m, 5H, CH_2) 1.41 (m, 5H, CH_2), 1.40 (m, 6H, CH2), 0.95 (t, 3H, CH_3).

Synthesis of nickel (III) butyl xanthate, Ni[S2COnBu]3 (Complex 1).

An aqueous solution of $NiNO_3.6H_2O$ (0.514 g, 1.77 mmol) (10 ml) was slowly added to a solution of P1 (1 g, 5.3 mmol) dissolved in distilled water (10 ml) while stirring. A green precipitate formed. The solution was stirred constantly at room temperature for 15 min. The green precipitate was washed with H_2O two times and dried under vacuum overnight. Yield: 0.80 g (89%). Elemental analysis for $C_{15}H_{27}NiO_3S_6$: found: C, 39.42%; H, 6.06%; S, 35.07%; Ni, 10.70%; calc. C, 40.08%; H, 6.46%; S, 36.72%; Ni, 10.02%. ES+ (m/z): [M+H] + 505.

Synthesis of nickel (III) pentyl xanthate, $Ni[S_2CO_nPn]_3$ (Complex 2).

Complex (2) was synthesized by the same method as complex (1) except using potassium pentyl xanthate [$K(S_2CO_nPn)$] (P2) instead of (P1). The product formed was a green solid. Yield: 0.68 g (77%), elemental analysis for $C_{18}H_{33}NiO_3S_6$: found: C, 35.58%; H, 5.37%; S, 37.98%; Ni, 11.59%; calc. C, 36.08%; H, 5.66%; S, 36.96%; Ni, 11.09%. ES+ (m/z): [M+H] + 549.

Declarations

Acknowledgements

The authors would like to thank the University Central Laboratory, College of Science and Humanities in Al-Kharj, Prince Sattam bin Abdulaziz University, Al-Kharj 11942, Saudi Arabia.

Author contributions statement

A.A, F.A, S.L and E.S. conducted the experiments, A.A, A.A, S.L and DS analyzed the results, A.A, S.l and DS write and revise the manuscript, A.A and A.A conceptualize and sort the work.

All authors reviewed the manuscript.

References

1. Gaponenko SV. Optical properties of semiconductor nanocrystals. Cambridge university press; 1998 Oct 28.
2. Leslie-Pelecky DL, Rieke RD. Magnetic properties of nanostructured materials. Chemistry of materials. 1996 Aug 14;8(8):1770-83.
3. Ying JY. Design and synthesis of nanostructured catalysts. Chemical Engineering Science. 2006 Mar 1;61(5):1540-8.
4. Murray C, Norris DJ, Bawendi MG. Synthesis and characterization of nearly monodisperse CdE (E= sulfur, selenium, tellurium) semiconductor nanocrystallites. Journal of the American Chemical Society. 1993 Sep;115(19):8706-15.
5. Chandran SP. New methods towards synthesis and controlled functionalisation of inorganic nanoparticles.
6. Wu PC, Ma RM, Liu C, Sun T, Ye Y, Dai L. High-performance CdS nanobelt field-effect transistors with high-κ HfO 2 top-gate dielectrics. Journal of Materials Chemistry. 2009;19(15):2125-30.
7. Ehlert O, Osvet A, Batentschuk M, Winnacker A, Nann T. Synthesis and spectroscopic investigations of Cu-and Pb-doped colloidal ZnS nanocrystals. The Journal of Physical Chemistry B. 2006 Nov 23;110(46):23175-8.
8. Quan Z, Wang Z, Yang P, Lin J, Fang J. Synthesis and characterization of high-quality ZnS, ZnS: Mn2+, and ZnS: Mn2+/ZnS (core/shell) luminescent nanocrystals. Inorganic chemistry. 2007 Feb 19;46(4):1354-60.
9. Chen X, Zhang X, Wan J, Wang Z, Qian Y. Selective fabrication of metastable greigite (Fe3S4) nanocrystallites and its magnetic properties through a simple solution-based route. Chemical Physics Letters. 2005 Feb 25;403(4-6):396-9.
10. Tilley RD, Jefferson DA. The synthesis of nickel sulfide nanoparticles on graphitized carbon supports. The Journal of Physical Chemistry B. 2002 Oct 24;106(42):10895-901.

11. Ghezelbash A, Korgel BA. Nickel sulfide and copper sulfide nanocrystal synthesis and polymorphism. Langmuir. 2005 Oct 11;21(21):9451-6.
12. Sigman MB, Ghezelbash A, Hanrath T, Saunders AE, Lee F, Korgel BA. Solventless synthesis of monodisperse Cu2S nanorods, nanodisks, and nanoplatelets. Journal of the American Chemical Society. 2003 Dec 24;125(51):16050-7.
13. Shombe GB, Khan MD, Zequine C, Zhao C, Gupta RK, Revaprasadu N. Direct solvent free synthesis of bare α-NiS, β-NiS and α-β-NiS composite as excellent electrocatalysts: Effect of self-capping on supercapacitance and overall water splitting activity. Scientific reports. 2020 Feb 24;10(1):1-4.
14. Sajjad M, Khan Y. Rational design of self-supported Ni 3 S 2 nanoparticles as a battery type electrode material for high-voltage (1.8 V) symmetric supercapacitor applications. CrystEngComm. 2021;23(15):2869-79.
15. Marand NA, Masoudpanah SM, Alamolhoda S, Bafghi MS. Solution combustion synthesis of nickel sulfide/reduced graphene oxide composite powders as electrode materials for high-performance supercapacitors. Journal of Energy Storage. 2021 Jul 1;39:102637.
16. Li J, Ding Z, Li J, Wang C, Pan L, Wang G. Synergistic coupling of NiS1. 03 nanoparticle with S-doped reduced graphene oxide for enhanced lithium and sodium storage. Chemical Engineering Journal. 2021 Mar 1;407:127199.
17. Li K, Yu J, Wang Q, Li L, Zhang W, Ma J, Zhang J, Liu P, Li D. Improved sodium storage properties of nickel sulfide nanoparticles decorated on reduced graphene oxide nanosheets as an advanced anode material. Nanotechnology. 2021 Feb 15;32(19):195406.
18. Kumari S, Chowdhury A, Khan AA, Hussain S. Controlled surface functionalization of Ni-S nanostructures for pH-responsive selective and superior pollutants adsorption. Journal of Hazardous Materials. 2021 Aug 5;415:125750.
19. Zhang W, Xing P, Zhang J, Chen L, Yang J, Hu X, Zhao L, Wu Y, He Y. Facile preparation of novel nickel sulfide modified KNbO3 heterojunction composite and its enhanced performance in photocatalytic nitrogen fixation. Journal of Colloid and Interface Science. 2021 May 15;590:548-60.
20. Dev S, Singh M. Metallic sulfide nanoparticles anchored graphene oxide: Synthesis, characterization and reduction of methylene blue to leuco methylene blue in aqueous mixtures. Journal of Physics and Chemistry of Solids. 2020 Apr 1;139:109335.
21. Lakshmanan P, Thirumaran S, Ciattini S. Synthesis, spectral and structural studies on NiS2PN and NiS2P2 chromophores and use of Ni (II) dithiocarbamate to synthesize nickel sulfide and nickel oxide for photodegradation of dyes. Journal of Molecular Structure. 2020 Nov 15;1220:128704.
22. Chung IM, Venkidasamy B, Thiruvengadam M. Nickel oxide nanoparticles cause substantial physiological, phytochemical, and molecular-level changes in Chinese cabbage seedlings. Plant Physiology and Biochemistry. 2019 Jun 1;139:92-101.
23. Natu G, Hasin P, Huang Z, Ji Z, He M, Wu Y. Valence band-edge engineering of nickel oxide nanoparticles via cobalt doping for application in p-type dye-sensitized solar cells. ACS applied materials & interfaces. 2012 Nov 28;4(11):5922-9.

24. Mola GT, Mthethwa MC, Hamed MS, Adedeji MA, Mbuyise XG, Kumar A, Sharma G, Zang Y. Local surface plasmon resonance assisted energy harvesting in thin film organic solar cells. Journal of Alloys and Compounds. 2021 Mar 5;856:158172.
25. Mun CH, Gopi CV, Vinodh R, Sambasivam S, Obaidat IM, Kim HJ. Microflower-like nickel sulfide-lead sulfide hierarchical composites as binder-free electrodes for high-performance supercapacitors. Journal of Energy Storage. 2019 Dec 1;26:100925.
26. ul Ain N, Aamir A, Khan Y, Rehman MU, Lin DJ. Catalytic and photocatalytic efficacy of hexagonal CuS nanoplates derived from copper (II) dithiocarbamate. Materials Chemistry and Physics. 2020 Feb 15;242:122408.
27. Buchmaier C, Glänzer M, Torvisco A, Poelt P, Wewerka K, Kunert B, Gatterer K, Trimmel G, Rath T. Nickel sulfide thin films and nanocrystals synthesized from nickel xanthate precursors. Journal of Materials Science. 2017 Sep;52(18):10898-914.
28. Al-Shakban M, Matthews PD, Savjani N, Zhong XL, Wang Y, Missous M, O'Brien P. The synthesis and characterization of Cu 2 ZnSnS 4 thin films from melt reactions using xanthate precursors. Journal of materials science. 2017 Nov;52(21):12761-71.
29. Gervas C, Mlowe S, Akerman MP, Ezekiel I, Moyo T, Revaprasadu N. Synthesis of rare pure phase Ni3S4 and Ni3S2 nanoparticles in different primary amine coordinating solvents. Polyhedron. 2017 Jan 28;122:16-24.
30. Ung D, Cossairt BM. Effect of surface ligands on CoP for the hydrogen evolution reaction. ACS Applied Energy Materials. 2019 Mar 1;2(3):1642-5.
31. Henckel DA, Lenz O, Cossairt BM. Effect of ligand coverage on hydrogen evolution catalyzed by colloidal WSe2. ACS Catalysis. 2017 Apr 7;7(4):2815-20.
32. Puthussery J, Seefeld S, Berry N, Gibbs M, Law M. Colloidal iron pyrite (FeS2) nanocrystal inks for thin-film photovoltaics. Journal of the American Chemical Society. 2011 Feb 2;133(4):716-9.
33. Xu C, Zeng Y, Rui X, Xiao N, Zhu J, Zhang W, Chen J, Liu W, Tan H, Hng HH, Yan Q. Controlled soft-template synthesis of ultrathin C@ FeS nanosheets with high-Li-storage performance. ACS nano. 2012 Jun 26;6(6):4713-21.
34. Steinhagen C, Harvey TB, Stolle CJ, Harris J, Korgel BA. Pyrite nanocrystal solar cells: promising, or fool's gold?. The Journal of Physical Chemistry Letters. 2012 Sep 6;3(17):2352-6.
35. Cao F, Hu W, Zhou L, Shi W, Song S, Lei Y, Wang S, Zhang H. 3D Fe 3 S 4 flower-like microspheres: high-yield synthesis via a biomolecule-assisted solution approach, their electrical, magnetic and electrochemical hydrogen storage properties. Dalton Transactions. 2009(42):9246-52.
36. Kar S, Chaudhuri S. Solvothermal synthesis of nanocrystalline FeS2 with different morphologies. Chemical Physics Letters. 2004 Nov 1;398(1-3):22-6.
37. Xuefeng Q, Yi X, Yitai Q. Solventothermal synthesis and morphological control of nanocrystalline FeS2. Materials Letters. 2001 Mar 1;48(2):109-11.
38. Anuar K, Tan WT, Saravanan N, Ho SM, Gwee SY. Influence of pH values on chemical bath deposited FeS2 thin films. Pacific J. Sci. Technol. 2009;10:801-5.

39. Larsen TH, Sigman M, Ghezelbash A, Doty RC, Korgel BA. Solventless synthesis of copper sulfide nanorods by thermolysis of a single source thiolate-derived precursor. Journal of the American Chemical Society. 2003 May 14;125(19):5638-9.
40. Chen J, Chen L, Wu LM. The solventless syntheses of unique PbS nanowires of x-shaped cross sections and the cooperative effects of ethylenediamine and a second salt. Inorganic chemistry. 2007 Sep 17;46(19):8038-43.
41. Abe K, Hanada T, Yoshida Y, Tanigaki N, Takiguchi H, Nagasawa H, Nakamoto M, Yamaguchi T, Yase K. Two-dimensional array of silver nanoparticles. Thin Solid Films. 1998 Aug 31;327:524-7.
42. Chen YB, Chen L, Wu LM. Structure-controlled solventless thermolytic synthesis of uniform silver nanodisks. Inorganic chemistry. 2005 Dec 26;44(26):9817-22.
43. Sigman MB, Korgel BA. Solventless synthesis of Bi2S3 (bismuthinite) nanorods, nanowires, and nanofabric. Chemistry of materials. 2005 Apr 5;17(7):1655-60.
44. Chen L, Chen YB, Wu LM. Synthesis of uniform Cu2S nanowires from Copper– thiolate polymer precursors by a solventless thermolytic method. Journal of the American Chemical Society. 2004 Dec 22;126(50):16334-5.
45. Ghezelbash A, Sigman MB, Korgel BA. Solventless synthesis of nickel sulfide nanorods and triangular nanoprisms. Nano Letters. 2004 Apr 14;4(4):537-42.
46. Chen J, Chen L, Wu LM. The solventless syntheses of unique PbS nanowires of x-shaped cross sections and the cooperative effects of ethylenediamine and a second salt. Inorganic chemistry. 2007 Sep 17;46(19):8038-43.
47. Jose D, Jagirdar BR. Synthesis and characterization of Pd (0), PdS, and Pd@ PdO core–shell nanoparticles by solventless thermolysis of a Pd–thiolate cluster. Journal of Solid State Chemistry. 2010 Sep 1;183(9):2059-67.
48. Thammakan N, Somsook E. Synthesis and thermal decomposition of cadmium dithiocarbamate complexes. Materials Letters. 2006 May 1;60(9-10):1161-5.
49. Revaprasadu N, Mlondo SN. Use of metal complexes to synthesize semiconductor nanoparticles. Pure and applied chemistry. 2006 Jan 1;78(9):1691-702.
50. Vittal JJ, Ng MT. Chemistry of metal thio-and selenocarboxylates: precursors for metal sulfide/selenide materials, thin films, and nanocrystals. Accounts of chemical research. 2006 Nov 21;39(11):869-77.
51. Fan D, Afzaal M, Mallik MA, Nguyen CQ, O'Brien P, Thomas PJ. Using coordination chemistry to develop new routes to semiconductor and other materials. Coordination chemistry reviews. 2007 Jul 1;251(13-14):1878-88.
52. Malik MA, Revaprasadu N, O'Brien P. Air-stable single-source precursors for the synthesis of chalcogenide semiconductor nanoparticles. Chemistry of materials. 2001 Mar 19;13(3):913-20.
53. Barrelet CJ, Wu Y, Bell DC, Lieber CM. Synthesis of CdS and ZnS nanowires using single-source molecular precursors. Journal of the American Chemical Society. 2003 Sep 24;125(38):11498-9.

54. Han W, Gao M. Investigations on iron sulfide nanosheets prepared via a single-source precursor approach. Crystal Growth and Design. 2008 Mar 5;8(3):1023-30.
55. Vanitha PV, O'Brien P. Phase control in the synthesis of magnetic iron sulfide nanocrystals from a cubane-type Fe– S cluster. Journal of the American Chemical Society. 2008 Dec 24;130(51):17256-7.
56. Geng B, Liu X, Ma J, Du Q. A new nonhydrolytic single-precursor approach to surfactant-capped nanocrystals of transition metal sulfides. Materials Science and Engineering: B. 2007 Dec 20;145(1-3):17-22.
57. Beal JH, Etchegoin PG, Tilley RD. Transition metal polysulfide complexes as single-source precursors for metal sulfide nanocrystals. The Journal of Physical Chemistry C. 2010 Mar 11;114(9):3817-21.
58. de Azeredo LC, da Silva VH, Marques MM, Ferreira GB, de Paula Machado S. Spectroscopic and Crystallographic Studies of the Complex tris (O-propyldithiocarbonate) cobalt (III). Journal of Molecular Structure. 2021 May 5;1231:129997.
59. Al-Shakban M, Matthews PD, O'Brien P. A simple route to complex materials: the synthesis of alkaline earth–transition metal sulfides. Chemical Communications. 2017;53(72):10058-61.
60. Roffey A, Hollingsworth N, Islam HU, Mercy M, Sankar G, Catlow CR, Hogarth G, de Leeuw NH. Phase control during the synthesis of nickel sulfide nanoparticles from dithiocarbamate precursors. Nanoscale. 2016;8(21):11067-75.
61. Buchmaier C, Glänzer M, Torvisco A, Poelt P, Wewerka K, Kunert B, Gatterer K, Trimmel G, Rath T. Nickel sulfide thin films and nanocrystals synthesized from nickel xanthate precursors. Journal of Materials Science. 2017 Sep;52(18):10898-914.
62. Almanqur L, Vitorica-yrezabal I, Whitehead G, Lewis DJ, O'Brien P. Synthesis of nanostructured powders and thin films of iron sulfide from molecular precursors. RSC advances. 2018;8(51):29096-103.
63. Fazli Y, Pourmortazavi SM, Kohsari I, Sadeghpur M. Electrochemical synthesis and structure characterization of nickel sulfide nanoparticles. Materials science in semiconductor processing. 2014 Nov 1;27:362-7.
64. Akhtar M, Revaprasadu N, Malik MA, Raftery J. Deposition of phase pure nickel sulfide thin films from bis (O-alkylxanthato)–nickel (II) complexes by the aerosol assisted chemical vapour deposition (AACVD) method. Materials Science in Semiconductor Processing. 2015 Feb 1;30:368-75.
65. Salavati-Niasari M, Banaiean-Monfared G, Emadi H, Enhessari M. Synthesis and characterization of nickel sulfide nanoparticles via cyclic microwave radiation. Comptes Rendus Chimie. 2013 Oct 1;16(10):929-36.
66. Yu SH, Yoshimura M. Fabrication of Powders and Thin Films of Various Nickel Sulfides by Soft Solution-Processing Routes. Advanced Functional Materials. 2002 Apr 18;12(4):277-85.

Figures

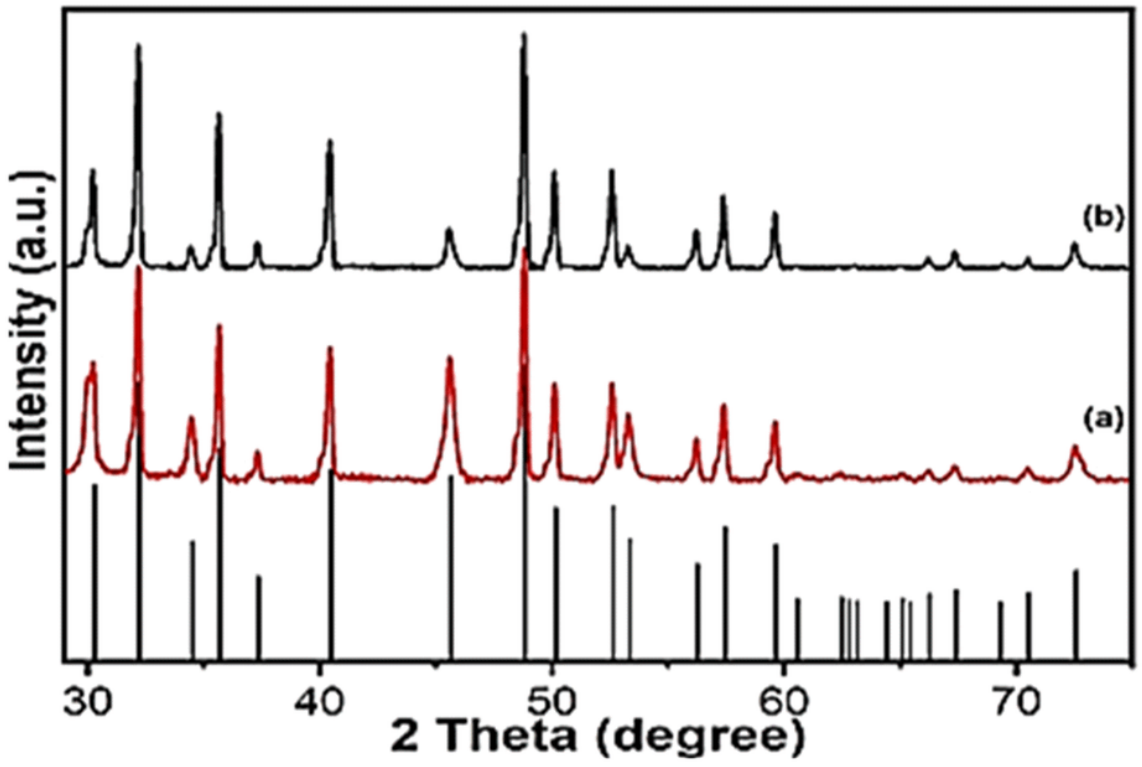

Figure 1

p.XRD for NiS nanoparticles (Complex 1) (COD no. 96-500-0115) obtained from precursor (1) at 400 oC (a) and 500 oC (b)

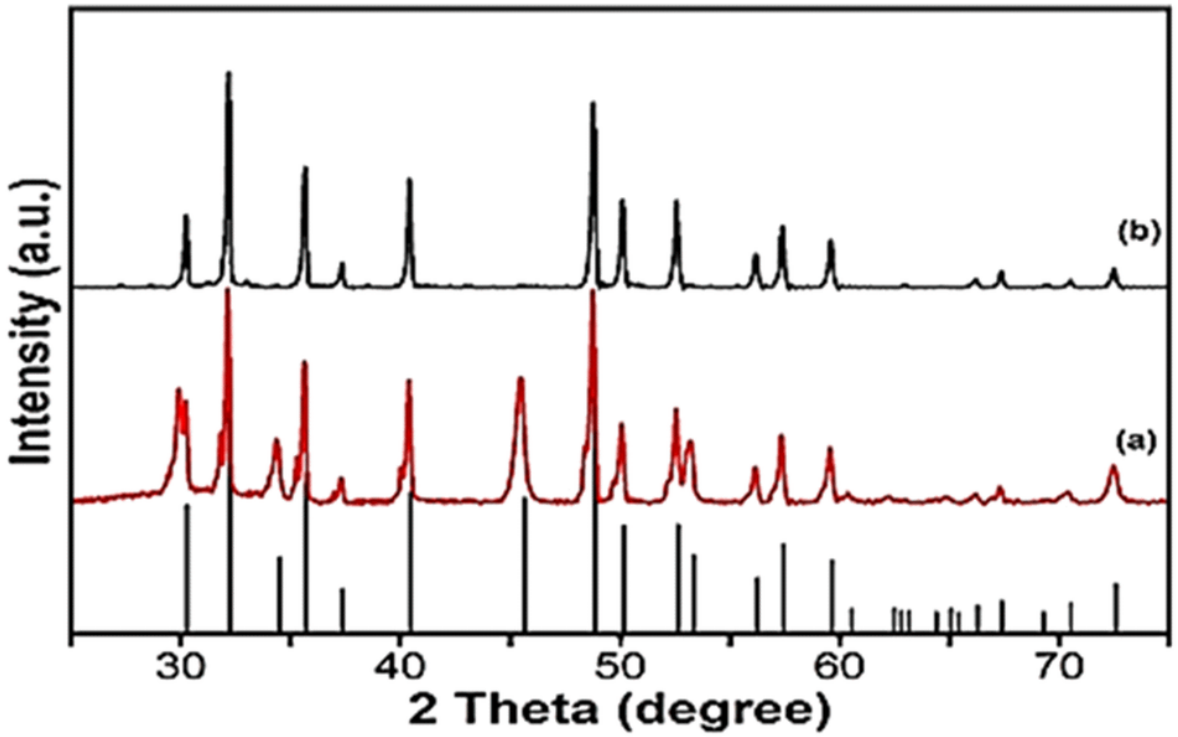

Figure 2

p.XRD for NiS nanoparticles (Complex 2) (COD no. 96-500-0115) obtained from precursor (2) at 400 oC (a) and 500 oC (b).

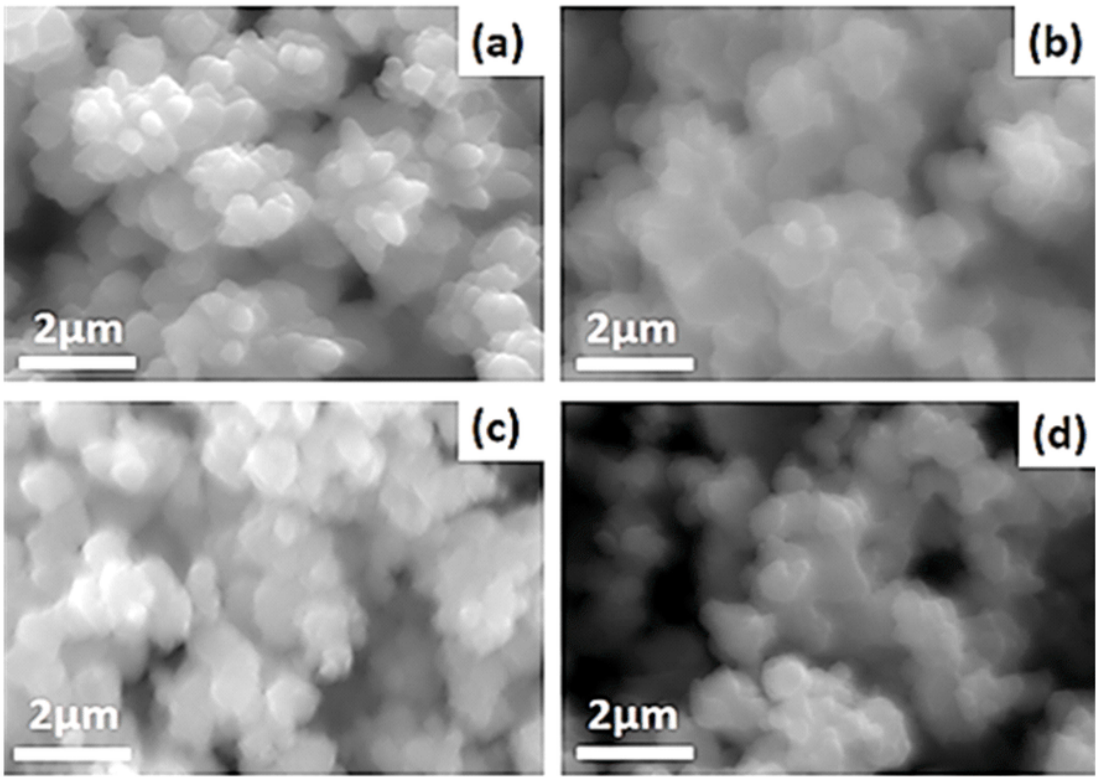

Figure 3

SEM images for NiS nanoparticles (COD no. 96-500-0115) from precursor (1) at 400 oC (a) and 500 oC (b). NiS obtained from precursor (2) at 400 oC (c) and 500 oC (d).

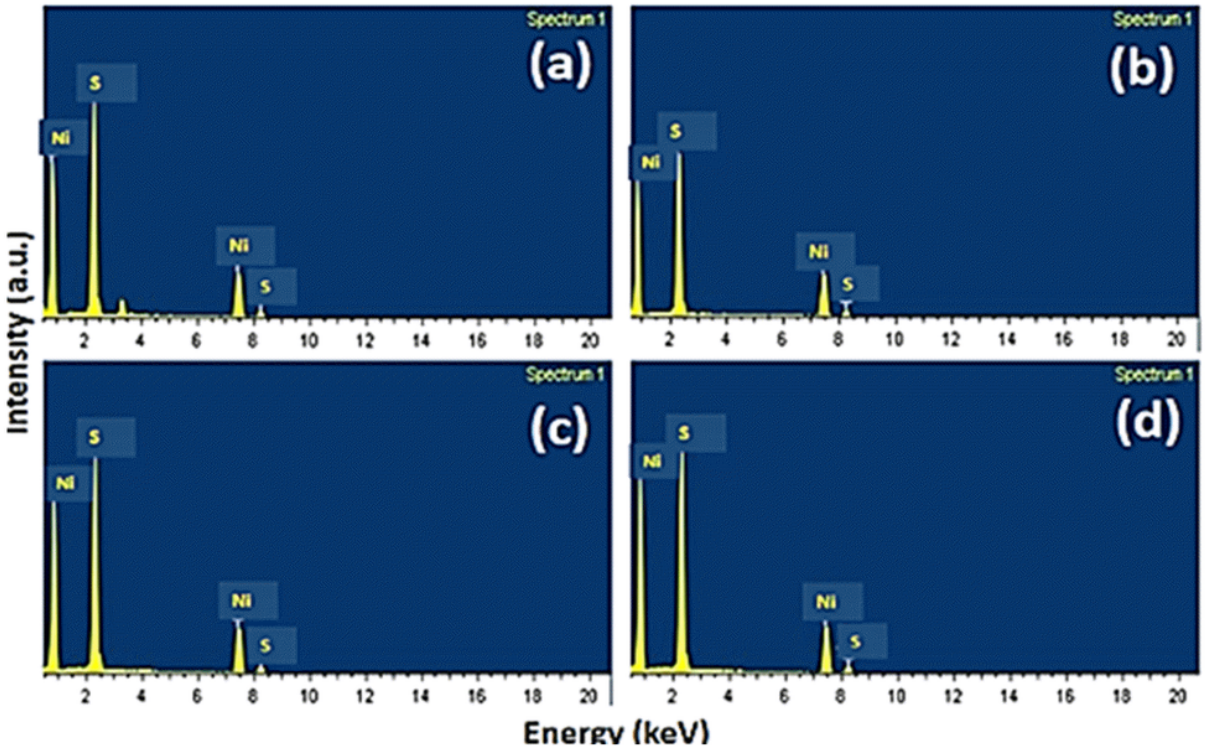

Figure 4

EDX for NiS nanoparticles (COD no. 96-500-0115) obtained from precursor (1) at 400 oC (a) and 500 oC (b). NiS obtained from precursor (2) at 400 oC (c) and 500 oC (d).